

AURKA, TOP2A and MELK are the key genes identified by WGCNA for the pathogenesis of lung adenocarcinoma

YUNQING XU^{1*}, SEN WANG^{2,3*}, BIN XU¹, HUIQING LIN⁴, NA ZHAN⁵, JIACAI REN⁵,
WENLING SONG¹, RONG HAN¹, LIPING CHENG¹, MAN ZHANG¹ and XIUYUN ZHANG⁵

¹Department of Oncology, People's Hospital of Huangpi District, Wuhan, Hubei 430000; ²Department of Forensic Medicine;

³School of Basic Medicine Sciences, Guangxi Medical University, Nanning, Guangxi 530021; Departments of

⁴Thoracic Surgery and ⁵Pathology, Renmin Hospital of Wuhan University, Wuhan, Hubei 430060, P.R. China

Received September 22, 2022; Accepted February 23, 2023

DOI: 10.3892/ol.2023.13824

Abstract. The comprehensive analysis of single or multiple microarray datasets is currently available in Gene Expression Omnibus (GEO) databases, with several studies having identified genes strongly associated with the development of lung adenocarcinoma (LUAD). However, the mechanisms of LUAD development remain largely unknown and has not yet been systematically studied; thus, further studies are required in this field. In the present study, weighted gene co-expression network analysis (WGCNA) was used for the evaluation of key genes with potential high risk of LUAD, and to provide more reliable evidence concerning its pathogenesis. The GSE140797 dataset from the high-throughput GEO database was downloaded and was first analyzed using the Limma package in the R language in order to determine the differentially expressed genes. The dataset was then analyzed using the WGCNA package to analyze the co-expressed genes, and the modular genes with the highest correlation with the clinical phenotype were identified. Subsequently, the pathogenic genes shared in common between the result of the two analyses were imported into the STRING database for protein-protein interaction network analysis. The hub genes were screened out using Cytoscape, and then The Cancer Genome Atlas analysis, receiver operating characteristic analysis and survival analysis were subsequently performed. Finally, the key genes were evaluated using reverse transcription-quantitative PCR and western blot analysis. Bioinformatics analysis of the GSE140797 dataset revealed eight key genes: *AURKA*, *BUB1*,

CCNBI, *CDK1*, *MELK*, *NUSAPI*, *TOP2A* and *PBK*. Finally, the *AURKA*, *TOP2A* and *MELK* genes were evaluated in samples from patients with lung cancer using WGCNA and RT-qPCR, western blot analysis experiments, providing basis for further research on the mechanisms of LUAD development and targeted therapy.

Introduction

Lung cancer is considered as one of the most lethal tumors, having the most increased incidence rate among tumors, with the highest mortality rate worldwide. Lung cancer remains the leading cause of cancer-related mortality, ranking first in percentage due to cancer in 2020 (1). According to the pathological type, lung cancer can be divided into small cell lung cancer and non-small cell lung cancer (NSCLC), of which NSCLC accounts for 80% of all, and lung adenocarcinoma (LUAD) accounts for the majority of NSCLC. The majority of patients with NSCLC, patients with LUAD in particular, exhibit symptoms not earlier than the middle or late stages of the disease, since the etiology remains unclear and early symptoms are not evident. In spite of several advancements being made in the treatment of LUAD, the average overall survival of patients with LUAD is limited to <5 years (2). Therefore, it is of utmost urgency to further identify novel key molecules for the development of novel therapeutic targets.

Several LUAD molecular markers have been identified in previous studies (3-7); however, a single gene cannot accurately represent the characteristics of LUAD due to its complex pathophysiology. Unlike the differential expression analysis that focuses on a single gene, co-expression network analysis provides new insight into understanding the pathogenesis of diseases and opportunities for therapeutic intervention by unsupervised identification of co-expressed gene modules (8,9). It has been successfully applied to the study of various biological processes, including chronic obstructive pulmonary disease and cancer, and has been proven to be quite effective in identifying candidate biological markers and therapeutic targets (9,10).

Currently, several studies have identified genes that are closely associated with LUAD development through comprehensive analysis of single or multiple microarray datasets

Correspondence to: Dr Xiuyun Zhang, Department of Pathology, Renmin Hospital of Wuhan University, 238 Jiefang Road, 99 Zhangzhidong Road, Wuchang, Wuhan, Hubei 430060, P.R. China
E-mail: zhangxiuyun0826@163.com

*Contributed equally

Key words: lung adenocarcinoma, weighted gene co-expression network analysis, key genes, protein-protein interaction network

in the currently available in the Gene Expression Omnibus (GEO) database. For example, Dong *et al* (11) identified aurora kinase A (*AURKA*) and DNA topoisomerase II alpha (*TOP2A*) as the two genes with the highest lymph node stage (N), which may be targets for the diagnosis and treatment of LUAD. Zhang *et al* (12) observed mitotic spindle-related features that may be used as independent prognostic indicators for patients with LUAD. Wang *et al* (13) observed that *TOP2A* may be one of the key protein-coding genes for LUAD possibly serving as a biomarker and therapeutic target for LUAD. Li *et al* (14) suggested that eight genes, including *TOP2A*, marker of proliferation Ki-67 (*MKI67*), platelet and endothelial cell adhesion molecule 1 (*PECAMI*), *CDK1*, secreted phosphoprotein 1 (*SPPI*), checkpoint kinase 1 (*CHEK1*), cyclin B1 (*CCNB1*), and ribonucleotide reductase regulatory subunit M2 (*RRM2*) may be novel pivotal genes closely associated with the progression and prognosis of LUAD. Wang *et al* (15) revealed that *CCNB1*, *BUB1* mitotic checkpoint serine/threonine kinase B (*BUB1B*), cell division cycle 20 (*CDC20*), TTK protein kinase (*TTK*) and mitotic arrest deficient 2 like 1 (*MAD2L1*) may be potential targets for the treatment of LUAD. Chen *et al* (16) demonstrated that 10 gene targets including *CDK1* and *CDC20* were associated with a poor prognosis of patients with lung cancer. Fan *et al* (17) suggested that *TOP2A*, G protein-coupled receptor kinase 5 (*GRK5*), sirtuin 7 (*SIRT7*), minichromosome maintenance complex component 7 (*MCM7*), EGFR and collagen type I alpha 2 chain (*COL1A2*) may be used as predictors for the diagnosis of LUAD. Guo *et al* (18) proposed that *TOP2A* and *UBE2C* were independent prognostic factors for LUAD. Regardless of the abundance of studies on this topic, the mechanisms responsible for the development of LUAD remain unclear and have not yet been systematically studied, with further studies required.

In the present study, the gene expression profile dataset, GSE140797, was acquired from the GEO database, containing gene expression data from 14 samples, including seven normal lung and seven LUAD tissues for analysis. Following normalized data preprocessing, the differentially expressed genes (DEGs) between the two sample sets were analyzed. Concurrently, weighted gene co-expression network analysis (WGCNA) was performed to construct a gene co-expression network of LUAD and identify co-expression modules. Subsequently, eight cancer tissue and eight adjacent tissue samples were collected from patients with LUAD and reverse transcription-quantitative PCR (RT-qPCR) and western blot analysis were performed, in order to verify the WGCNA analysis, and the expression analysis of the three key genes, *AURKA*, *TOP2A* and maternal embryonic leucine zipper kinase (*MELK*), was evaluated.

AURKA is a cyclin whose activation is required for the process of cell division through the regulation of mitosis. The ectopic overexpression of the *AURKA* gene results in the inactivation of the G2-phase DNA damage checkpoint and the mitotic spindle assembly checkpoint, as well as tetraploid and centrosome expansion, particularly in cells with defective p53-dependent DNA damage checkpoints upstream of *AURKA*. At the transporter level, the EGF-induced expression of *AURKA* is dependent on the interaction of nuclear EGFR and STAT5. At the downstream end of *AURKA*, certain

substrates of *AURKA* play critical inhibitory roles, with p53 and large tumor suppressor kinase 2 being the most important substrates of *AURKA*. *AURKA* substrates have received widespread attention as tumor suppressors (19).

TOP2A has been demonstrated to be related to the progression of several cancer types, such as hepatocellular carcinoma (20), breast cancer (21), bladder cancer (22), ovarian cancer (23), cervical cancer (24), pancreatic cancer (25), stomach cancer (26), including NSCLC (27,28).

Increased expression of *MELK* has been observed in various cancer cells and tissues, playing a crucial and critical role in the proliferation and self-renewal of progenitor and tumor stem cells and is overexpressed in LUAD, increasing the probability of tumorigenesis. Among them, *MELK* increases the proliferation of cervical, breast, colorectal and pancreatic cancer cell lines (29), while it is also involved in and affects the development of hepatocellular carcinoma (30) and bladder cancer (31).

Materials and methods

Data source and preprocessing. GSE gene expression profile data and clinical information were obtained from the GEO database at the National Center for Bioinformatics. Gene expression data from 14 samples in the GSE140797 dataset were analyzed, including seven normal lung tissue and seven LUAD tissue samples. The annotation information of the GPL13497 (Agilent-026652 Whole Human Genome Microarray 4x44Kv2) platform was used as a reference to convert the probe to the corresponding gene symbol, and the Limma software (version 3.54.2) package was used to normalize the data for further analysis.

DEG analysis. The samples were divided into the normal control and LUAD groups, and the conditions $\log_2FC > 1$ and $P < 0.05$ were set to screen for genes with significant differences in expression.

Data filtering. Co-expression networks were constructed using the WGCNA package in the R language. To obtain a valid co-expression network, the expression variance of each gene in all samples was calculated, and the genes with the same variance were considered for the construction of the co-expression network. Cluster analysis was performed, in order to detect and remove outliers.

Construction of gene co-expression network. Scale-free networks were constructed by selecting an appropriate weighting coefficient (soft threshold) to make the connections between genes adhere to the scale-free distribution of network connection requirements, and the correlation coefficient between genes was used to construct hierarchical clustering tree. Different branches of the clustering tree represented different gene modules, and different colors represented different gene modules. Subsequently, genes were categorized according to their expression patterns based on their weighted correlation coefficients. The genes that exhibited similar gene expression patterns were then grouped into a module, and then classified by gene expression pattern for further analysis. Lastly, by applying this coefficient, the correlation matrix was

Table I. Oligonucleotide primers used in the present study.

Gene		Oligonucleotide primer sequence (5'-3')
GAPDH	Sense	GGAAGCTTGTTCATCAATGGAAATC
	Antisense	TGATGACCCTTTTGGCTCCC
CDK1	Sense	AAGGGTAGACACAAAACACTACAGGTC
	Antisense	ATGTACTGACCAGGAGGGATAGA
TOP2A	Sense	CCTTCTATGGTGGATGGTTTGA
	Antisense	ATGGGCTGCAAGAGGTTTAGAT
MELK	Sense	GATGTTCCCAAGTGGCTCTCTC
	Antisense	TCCTCCATTGTTTGCCTGTTG
NUSAP1	Sense	CTGCTGCTGTTATTACCCCATTC
	Antisense	CTTTCTTCTCCTTTTCGTTCTTGC
BUB1	Sense	GAAGAAATACCACAATGACCCAAG
	Antisense	TGGGTTTCAGTGAGGCGTGT
AURKA	Sense	TGCCCTGTCTTACTGTCATTCTG
	Antisense	AAAGGAGGCTTCCCAACTAAAA
CCNB1	Sense	GCCTATTTTGGTTGATACTGCCTC
	Antisense	CTCCATCTTCTGCATCCACATC
PBK	Sense	TGACTGCTCCTGCCTTCATAAC
	Antisense	TAACACCATTCTCCTCCACAGC

CDK1, cyclin dependent kinase 1; TOP2A, DNA topoisomerase II alpha; MELK, maternal embryonic leucine zipper kinase; NUSAP1, nucleolar and spindle associated protein 1; BUB1, BUB1 mitotic checkpoint serine/threonine kinase B; AURKA, aurora kinase A; CCNB1, cyclin B1; PBK, PDZ binding kinase.

converted into an adjacency matrix, which was then converted into a topological overlap matrix.

Module and clinical feature correlation analysis. The Pearson's correlation coefficients and P-values of the matrices composed of gene and sample and clinical correlations per module were calculated using WGCNA, and the Pearson's correlation coefficients were used to measure the correlation between different modules and clinical traits, and the module with the highest correlation coefficient was used in subsequent analysis. The correlation between gene expressed in the module and the phenotype [gene significance (GS)] and the correlation between gene expressed in the module and the module membership (MM) were analyzed, and the genes were screened according to GS >0.8 and MM >0.8.

Functional enrichment analysis. The cross section of modules with the highest correlation between WGCNA and DEGs were selected, and Kyoto Encyclopedia of Genes and Genomes (KEGG) and Gene Ontology (GO) analyses were performed on this part of the gene set using the R package cluster profiler (<https://www.bioconductor.org/packages/release/bioc/html/clusterProfiler.html>).

Construction of protein-protein interaction (PPI) networks. The STRING database (<https://string-db.org/>) was used to select intersecting genes to construct the PPI network. PPI pairs in the network were visualized with a combined confidence score of ≥ 0.4 . Hub genes in the PPI network were identified using cytohubba, a plug-in for Cytoscape software

(version 3.7.2. <https://cytoscape.org/>) that identifies the top 10 hub genes.

Verification of the central gene. The Gene Expression Profiling Interactive Analysis Database (<http://gepia.cancer-pku.cn/>) (32) is an online analysis tool which can be used to validate the top 10 central genes selected through protein-protein interaction networks, which are based on The Cancer Genome Atlas (TCGA) of Lung Adenocarcinoma (33) and the Genotype-Tissue Expression (GTEx) LUAD database, which provides differential expression analysis, profiling, and survival analysis for central gene expression analysis, receiver operating characteristic (ROC) curve analysis, and survival analysis.

Collection and processing of clinical tissue samples. A total of eight fresh frozen clinical samples were obtained from lung adenocarcinoma patients in Renmin Hospital of Wuhan University. In addition, three male and five female patients, ranging in age from 51 to 80 years, were recruited between December 14 and December 28, 2020. The specific age, sex, and disease stage were i) male 70 years old, 2020.12.14, IIB stage; ii) male 63 years old, 2020.12.16, IA2 stage; iii) female 62 years old, 2020.12.16, IA stage; iv) female 59 years old, 2020.12.16, A stage; v) male 51 years old, 2020.12.17, A stage; vi) female 80 years old, 2020.12.24, IA3 stage; vii) Female 73 years old, 2020.12.25, IA stage; viii) female 73 years old, 2020.12.28, IA stage). The samples were obtained with patient consent and ethical approval (approval no.WDRY2022-K231) from Renmin Hospital of Wuhan University (Wuhan, China).

RT-qPCR. RNA was obtained from frozen fresh samples of lung cancer and normal paracancerous lung tissue from eight lung adenocarcinoma patients. RNA extraction was conducted using TRIzol® reagent (cat. no. 15596026, Invitrogen; Thermo Fisher Scientific, Inc.) and reverse transcribed into cDNA using the PrimeScript RT Reagent kit according to the manufacturer's instructions (cat. no. RR037A; Takara Bio, Inc.). Candidate primers for each gene were designed using Premier 5 design program (PREMIER Biosoft). PCR reaction was performed with the quantitative TB Green-based PCR kit (cat. no. RR420A; Takara Bio, Inc.) using a CFX Connect PCR machine (CFX Connect TM; Bio-Rad Laboratories, Inc.). The following conditions were applied: Pre-denaturation stage: 95°C, 1 min for 1 cycle; amplification stage: denaturation at 95°C, 5 sec and annealing at 58°C, 30 sec, 40 cycles; melting curve stage: 65°C to 95°C, increment 0.5°C for 5 second. The results were analyzed using the $2^{-\Delta\Delta C_q}$ method (34), and the primer pair sequences for each gene are listed in Table I.

Western blot analysis. Western blot analysis of relative protein expression levels was performed as described as follows: Lung adenocarcinoma and parapulmonary carcinoma were lysed with RIPA (cat. no. P0013B; Beyotime Institute of Biotechnology) buffer to extract total proteins, and the protein concentrations were then detected using a BCA kit (cat. no. P0012S; Beyotime Institute of Biotechnology). The protein samples were denatured in a dry heater at 95°C and subsequently subjected to electrophoresis; 10% SDS gel (cat. no. P0012A; Beyotime Institute of Biotechnology) was used for electrophoresis and 25 µg of protein was loaded in each strip. Following electrophoresis, the separated proteins were transferred to polyvinylidene difluoride membranes (cat. no. FFP2; Beyotime Institute of Biotechnology) by the wet transfer membrane method. Non-specific proteins on the membrane were blocked for 1 h at room temperature and then incubated with primary monoclonal antibodies corresponding to the proteins overnight at 4°C. The antibodies used are as follows: A rabbit anti-AURKA polyclonal antibody (cat. no. A15728), a rabbit anti-BUB1 mitotic checkpoint serine/threonine kinase (BUB1) polyclonal antibody (cat. no. A1929), a rabbit anti-CCNB1 polyclonal antibody (cat. no. A16800), a rabbit anti-CDK1 polyclonal antibody (cat. no. A0220), a rabbit anti-MELK monoclonal antibody (cat. no. A3530), a rabbit anti-nucleolar and spindle associated protein 1 (NUSAP1) polyclonal antibody (cat. no. A16000), a rabbit anti-TOP2A polyclonal antibody (cat. no. A16440) and a mouse monoclonal antibody for β-actin (cat. no. AC004) (all from ABclonal Biotech Co., Ltd. and all at 1:1,000).

The following day, the membranes were incubated for 1 h at room temperature using the corresponding secondary antibody; Goat Anti-Rabbit IgG H&L (HRP; cat. no. ab205719) and Goat Anti-Mouse IgG H&L (HRP; cat. no. ab205719) all from Abcam and all at 1:10,000. This was followed by a brief incubation with ECL Western Blotting Detection Reagent (cat. no. P0018S; Beyotime Institute of Biotechnology) and a final exposure with an iBright imaging system (Thermo Fisher Scientific, Inc.). Density measurement was by ImageJ (version V1.8.0.112; National Institutes of Health).

Statistical analysis. For the statistical calculations, the R (version 3.6) and WGCNA packages were used. The calculation of the correlation coefficient between the relevant clinical characteristics of LUAD tissue and the ME of each co-expression module used in this article was based on the R language platform Rstudio (version 8.9.173593; <https://support--rstudio-com.netlify.app/products/rstudio/download/>). WGCNA was used to identify genes with similar functions. For each gene pair, WGCNA determines the likelihood of association by using a soft threshold. A weighted network of co-expression was formed based on this concept. The data are expressed as the mean ± SE. Parametric data were analyzed using the Student's paired t-test and non-parametric data were analyzed using the Mann-Whitney U test. $P < 0.05$ was considered to indicate a statistically significant difference.

Results

Data filtering. A co-expression network was constructed by including 5,435 genes with 25% of the maximum variation in the present study. No significant outliers were observed by building hierarchical clustering trees for 5,435 genes from 14 lung tissue samples. A total number of 580 DEGs were identified in the dataset (Fig. 1), among which 254 genes were downregulated and 326 genes were upregulated.

Construction of the gene co-expression network module. According to the non-scale network distribution fitting, a value of 20 was selected as the soft threshold (β value) for this dataset and a co-expression network was constructed (Fig. 2) for module identification using the dynamic cut tree method, finally acquiring 10 modules (Fig. 3A).

Correlation analysis of modules and clinical characteristics. By applying the correlation analysis of each module using sample clinical information, the green module presented with the highest positive correlation, and the blue module the highest degree of negative correlation with LUAD (Fig. 3B).

Identification and analysis of pivotal genes. According to the criteria of GS > 0.8 and MM > 0.8 to screen the key genes in the blue module and the green module for the following research stage, 845 and 285 key genes were selected from the blue and green modules, respectively. Subsequently, GO function enrichment analysis and KEGG enrichment analysis were performed on the 845 genes selected from blue module and the 285 genes selected from green module (Fig. 4A and B). As regards the green module, GO functional enrichment analysis revealed that common pathogenic genes were mainly enriched in mitotic cell cycle phase transition, cell cycle phase transition and cytoplasmic division, whereas in the blue module, the common pathogenic genes were mainly enriched in blood vessel development, blood vessel morphogenesis and angiogenesis (Fig. 4C). KEGG pathway analysis mainly demonstrated enrichment in the cell cycle, p53 signaling pathway and Fanconi anemia pathway in the green module, and proteoglycans in cancer, alcoholism and axon guidance in the blue module (Fig. 4D).

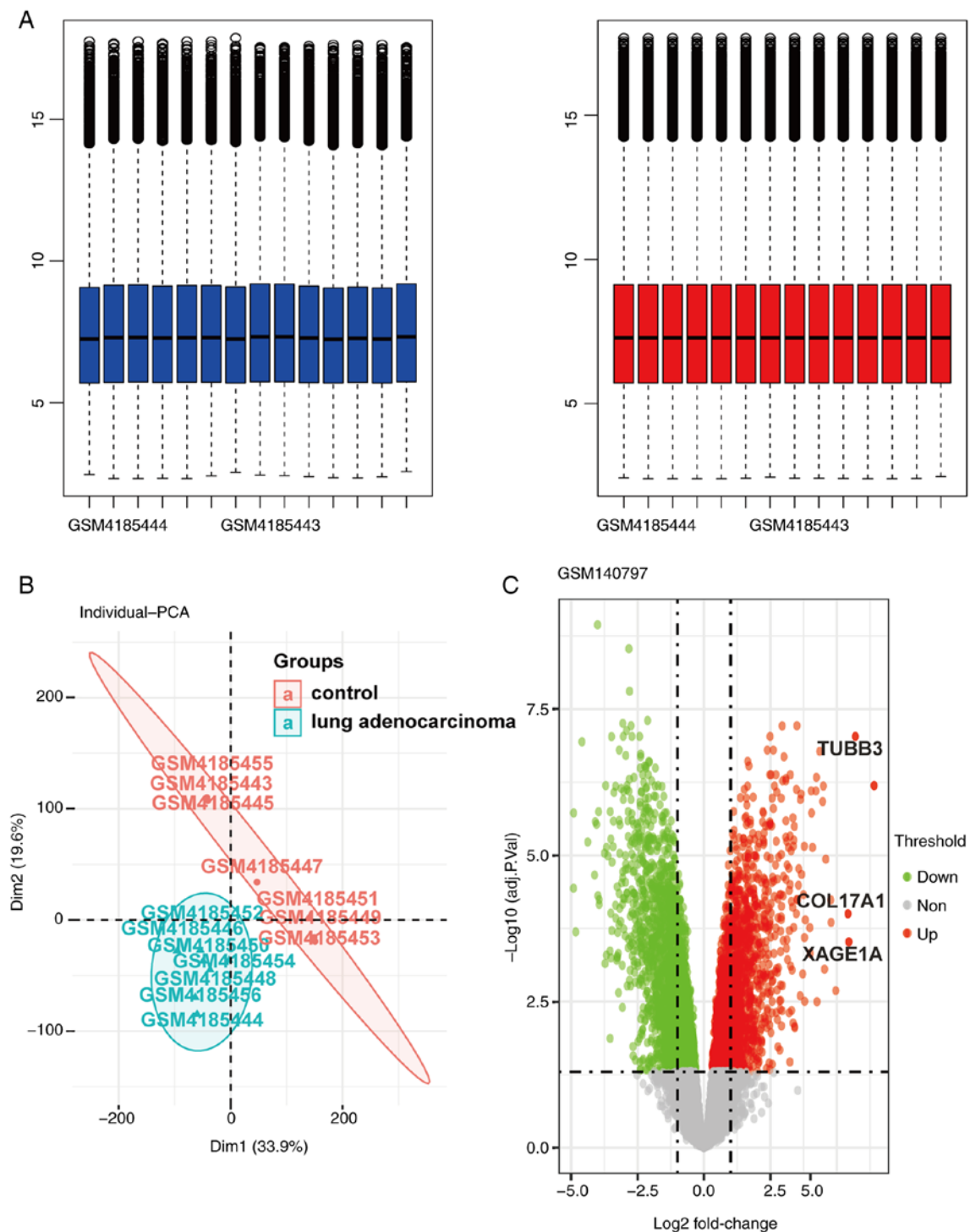


Figure 1. Normalization of gene expression and gene differential expression of data between two groups of samples. (A) Standardization of data. The blue bars represent the data before normalization, and the red bars represent the data following normalization. (B) Principal component analysis of two groups of sample data. (C) Differential expression of data between the two groups of samples. Red dots indicate upregulated genes and green dots indicate downregulated genes (lfold change>2.0, adj-P<0.05). Gray dots indicate genes with no significant difference in expression.

PPI network construction and analysis. The 845 genes from the blue module and 580 differentially expressed genes were intersected, in order to obtain 324 genes. Similarly, the 285 genes from the green module and 580 differential genes were intersected to obtain 107 genes. The two PPI networks for the aforementioned 324 and 107 genes were then respectively established using Cytoscape software (Fig. 5), and 10 key genes were selected from the two PPI networks, respectively according to

the degree of connectivity, including *AURKA*, *BUB1*, *CCNB1*, *CDC45*, *CDK1*, *MELK*, *NUSAP1*, *PBK*, *TOP2A*, *TTK*, *BDKRB2*, *CCL19*, *CX3CR1*, *CXCL13*, *CXCL9*, *CXCR4*, *CXCR5*, *GNAI1*, *GNG11* and *NMUR1*. Among the genes, *BDKRB2*, *CCL19*, *CX3CR1*, *CXCL13*, *CXCL9*, *CXCR4*, *CXCR5*, *GNAI1*, *GNG11* and *NMUR1* were selected from the blue module, with *AURKA*, *BUB1*, *CCNB1*, *CDC45*, *CDK1*, *MELK*, *NUSAP1*, *PBK*, *TOP2A* and *TTK* selected from the green module.

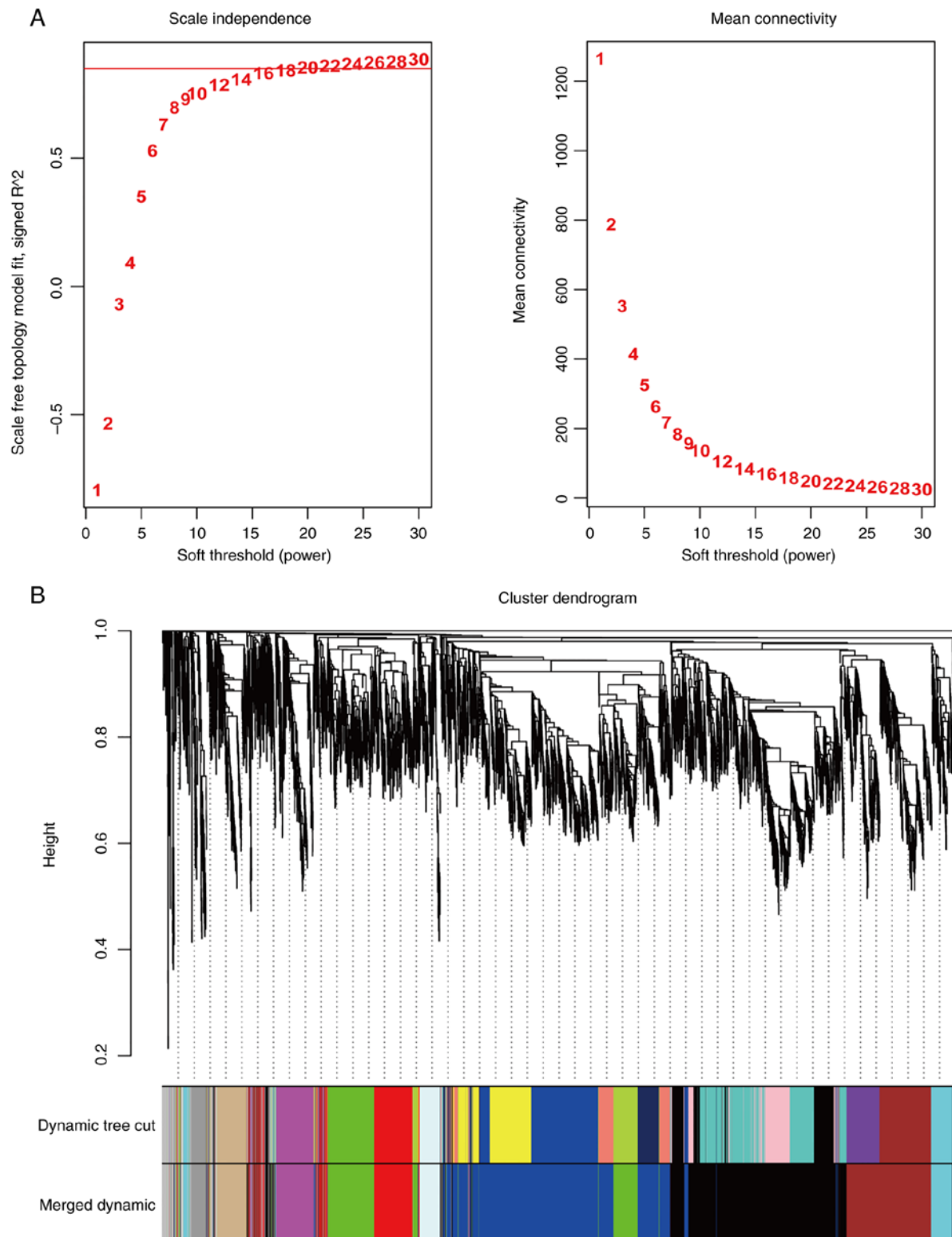


Figure 2. WGCNA analysis of the data. (A) Determination of the optimal soft thresholding power. (B) Construction of co-expression matrix and module visualization. WGCNA weighted gene co-expression network analysis. WGCNA, weighted gene co-expression network analysis.

Verification of the expression of the 20 selected genes in TCGA database. Subsequently, the expression profiles of 59 normal lung tissues and 515 LUAD tissues were acquired from TCGA database to verify the expression of the aforementioned 20 key genes. With the exception of the expression of *CXCR4* among the 20 genes, the expression of the remaining 19 genes

differed significantly between normal lung tissue and LUAD tissues (Fig. 6).

ROC curve analysis. Subsequently, ROC curve analysis was performed on the 19 genes verified in TCGA database, and it was observed that apart from *BDKRB2*, *CCL19*, *CXCR5*,

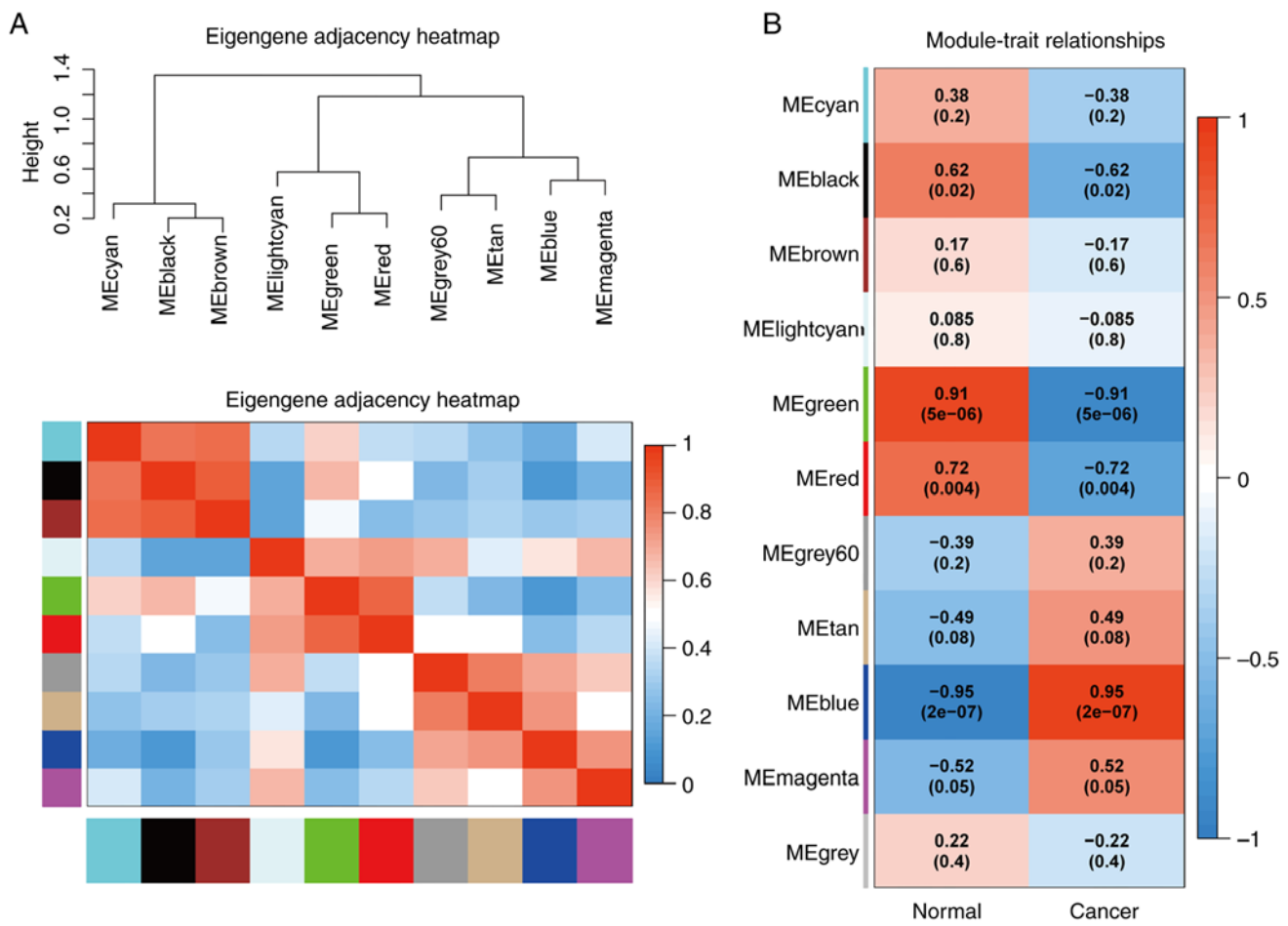


Figure 3. Module correlation analysis. (A) Correlation analysis between modules. The poor correlation between modules indicates that the module division is successful. (B) Correlation analysis between modules and diseases. The green module negatively correlated with disease ($R^2=0.91$; $P=5 \times 10^{-6}$), while the blue module positively correlated with disease ($R^2=0.95$; $P=2 \times 10^{-7}$).

CXCL9, *GNAL1* and *CX3CR1*, and the other 13 genes had AUCs >0.9 (Fig. 7) and were considered in the following stages of the analysis.

Survival analysis. Subsequently, survival analysis using the 13 genes was performed by GEPIA and it was determined that the P-value of eight genes was <0.05, including *AURKA*, *BUB1*, *CCNB1*, *CDK1*, *MELK*, *NUSAP1*, *PBK* and *TOP2A* (Fig. 8), indicating that they may be key genes that reduce lung adenocarcinoma survival and affect prognosis and were included in the following analysis.

Gene expression in human LUAD and normal paracancerous tissues. To validate the results of bioinformatics analysis, the expression levels of the aforementioned eight genes were verified in human LUAD tissues and paired lung paracancerous tissues using RT-qPCR and western blot analysis. The relative mRNA expression levels of seven out of eight genes, namely *AURKA*, *BUB1*, *CCNB1*, *CDK1*, *MELK*, *NUSAP1* and *TOP2A*, were significantly higher in the LUAD than in the adjacent normal lung tissues (Fig. 9). The protein levels of three out of these seven overexpressed genes, including *AURKA*, *MELK* and *TOP2A*, were significantly higher in the LUAD than in adjacent normal lung tissues (Fig. 10).

Discussion

Lung cancer is one of the most prevalent types of cancer and currently presents with the highest mortality rate. Among patients recently diagnosed with lung cancer, the 5-year survival rate following diagnosis has been observed to be extremely reduced in the majority of countries, with a survival rate of only 1/10 to 1/5 (35). However, the molecular mechanisms underlying LUAD remain poorly understood. Without early diagnosis, the majority of patients are not treated promptly, resulting in a very poor prognosis. Therefore, there is an urgent need for the identification of efficient biomarkers for the early detection and treatment of lung cancer. The screening of early biomarkers and key genes for malignant and benign diseases using bioinformatics analysis has been proven a very efficient method (36-39). However, the procedure of data analysis in a scientifically sound and efficient manner is currently a serious hindrance. In the present study, the information extracted from a high-throughput gene expression dataset was analyzed, firstly sorting the differentially expressed genes, and WGCNA was then used to obtain the genes in the modules with the highest correlation with the clinical phenotype. Subsequently, PPI and correlation analyses were performed on the common pathogenic genes of the two analyses.

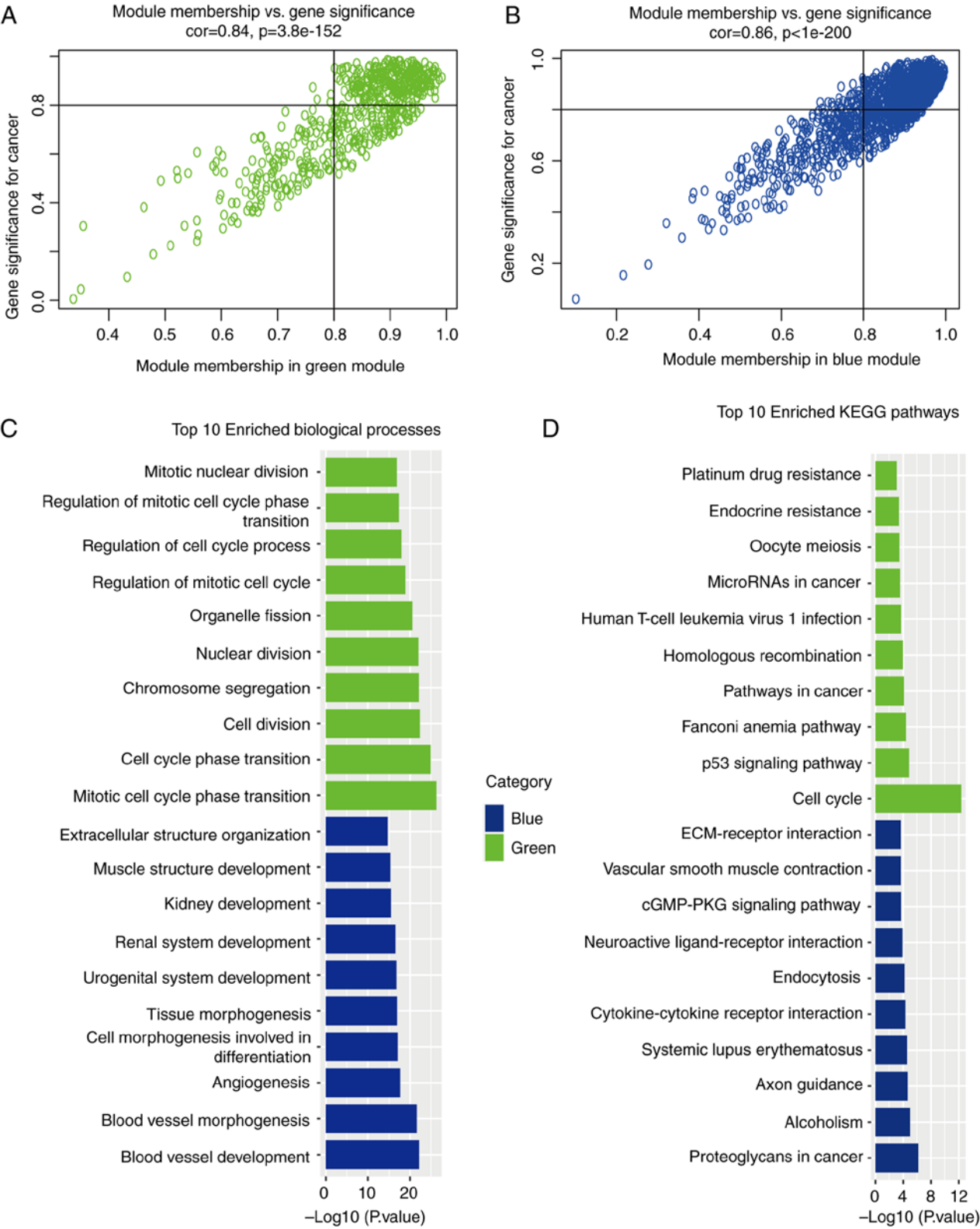


Figure 4. Correlation analysis between genes and traits for the green and blue modules. (A) Module membership vs. gene significance map of genes for green module. Hub genes with GS >0.8 and MM >0.8 were selected. (B) Module membership vs. gene significance map of genes for the blue module. Hub genes with GS >0.8 and MM >0.8 were selected. (C) The top 10 biological processes of hub gene enrichment analysis for the green module and blue modules. (D) Hub gene KEGG enrichment analysis of the top 10 pathways for the green and blue modules. GS, gene significance; MM, module membership; KEGG, Kyoto Encyclopedia of Genes and Genomes.

Several inhibitors with high specificity for *AURKA* have been developed with clinical efficacy, including MLN8237 and ENMD-2076 (40). Moreover, cell cycle inhibition by

regulating the *AURKA*/ polo-like kinase 1 (PLK1) pathway has been reported to induce apoptosis in LUAD (41), with *AURKA* not only being a potential biomarker for predicting

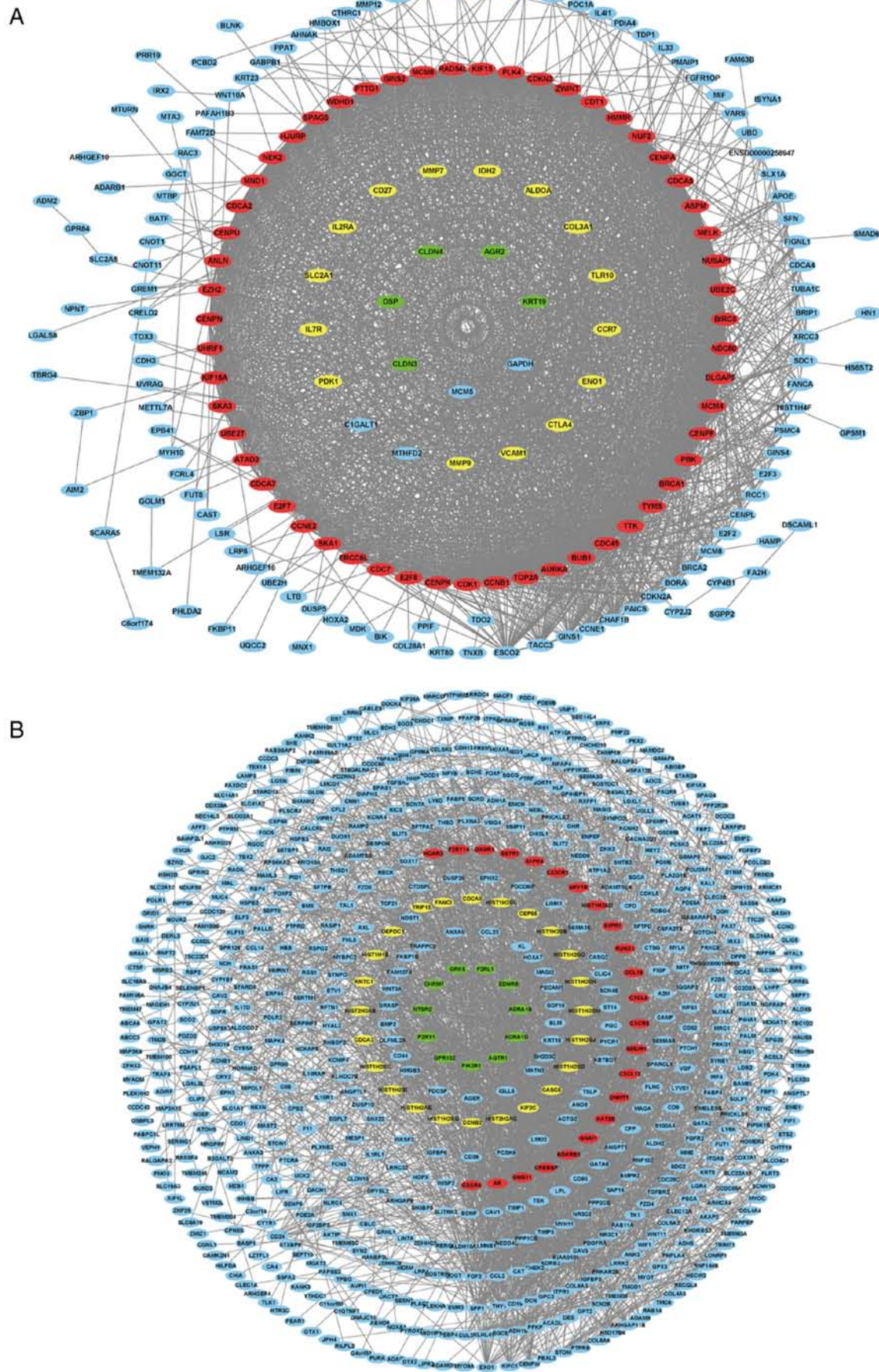


Figure 5. PPI analysis of all Hub genes in the green and blue modules. (A) PPI analysis of Hub gene for the green module. Red, yellow and green are the top three protein-protein interaction subnetworks respectively. (B) PPI analysis of hub genes for the blue module. Red, yellow and green are the top three PPI subnetworks respectively. PPI, protein-protein interaction.

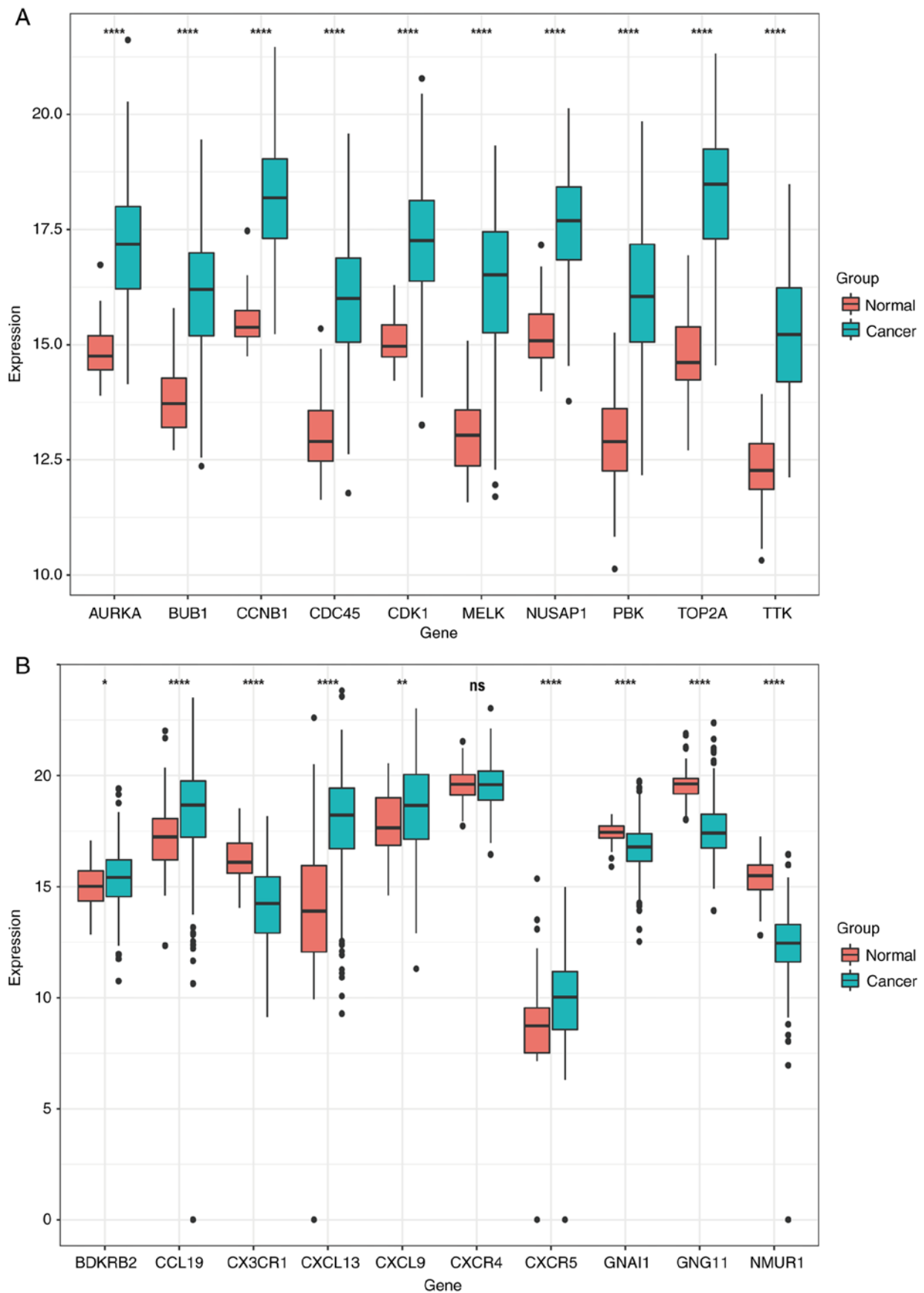


Figure 6. In total, 59 control samples and 504 cancer samples were derived from TCGA database for verification. From the 10 genes selected from the two modules, a total of 20 genes were verified. A total of 19 of these changes were verified, and the other one (*CXCR4*) was excluded. (A) The expression of *AURKA*, *BUB1*, *CCNB1*, *CDC45*, *CDK1*, *MELK*, *NUSAP1*, *PBK*, *TOP2A* and *TTK* genes in normal lung tissues and lung adenocarcinoma tissues, where red indicates normal lung tissues and green indicates lung adenocarcinoma tissues. (B) The expression of *BDKRB2*, *CCL19*, *CX3CR1*, *CXCL13*, *CXCL9*, *CXCR4*, *CXCR5*, *GNAI1*, *GNG11* and *NMUR1* genes in normal lung tissues and lung adenocarcinoma tissues, with red indicating normal lung tissues and green indicating lung adenocarcinoma tissues. t-test of normal lung tissue and lung adenocarcinoma tissue. * $P < 0.05$, ** $P < 0.01$ and **** $P < 0.0001$.

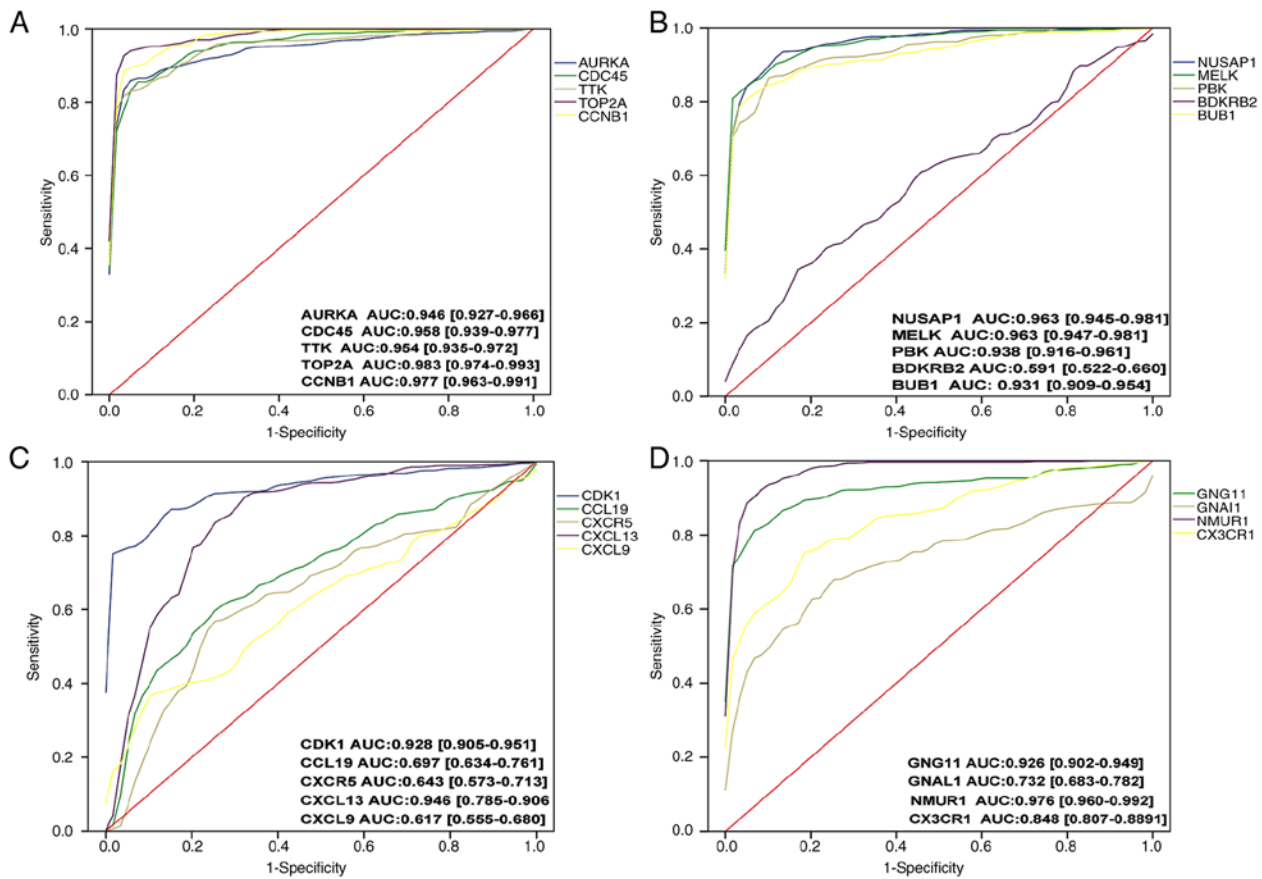


Figure 7. ROC curve analysis of 20 genes. AUCs >0.9 were included in the subsequent analysis. A total of 13 genes (*AURKA*, *CDC45*, *TTK*, *TOP2A*, *CCNB1*, *NUSAP1*, *MELK*, *PBK*, *BUB1*, *CDK1*, *CXCL13*, *GNG11* and *NMUR1*) were included, and seven genes were excluded. (A) ROC curve analysis was performed for the *AURKA*, *CDC45*, *TTK*, *TOP2A* and *CCNB1* genes sequentially. (B) ROC curve analysis was performed for the *NUSAP1*, *MELK*, *PBK*, *BKPB2* and *BUB1* genes sequentially. (C) ROC curve analysis was performed for the *CDK1*, *CCL19*, *CXCR5*, *CXCL13* and *CXCL9* genes sequentially. (D) ROC curve analysis was performed for the *CXCR4*, *GNG11*, *GNAL1* and *NMUR1*, *CX3CR1* genes sequentially. ROC, receiver operating characteristic; AUC, area under the curve.

the poor prognosis of smoking-related LUAD. Furthermore, the *AURKA* rs1047972 variant has been found to be significantly associated with EGFR mutation in patients with LUAD, particularly in women and non-smoking patients. The *AURKA* variant may contribute to the pathologic development of LUAD (42-44). The *AURKA*-induced amplification or activation of liver kinase B1 (LKB1)/AMPK signaling pathway impairment contributes to the initiation and progression of NSCLC, suggesting that *AURKA* may be a potential therapeutic target against *AURKA*-driven overactive LUAD (45).

Chemotherapy resistance research has emerged as a major challenge in cancer treatment. Currently, resistance to radiation therapy in LUAD has been attributed to elevated levels of autophagy and thus resistance, and *AURKA* is critical for the reduction chemotherapy resistance in LUAD, as evidenced by high levels of *AURKA* expression associated with chemoresistance and proliferation in LUAD. Genetic resistance in response to chronic EGFR inhibition attenuates drug-induced apoptosis, and silencing *AURKA* reduces drug resistance in EGFR-mutant LUAD (46,47).

It has been reported that *TOP2A* expression levels are upregulated in both surgically resected lung cancer tissues and lung cancer cell lines. As previously demonstrated, the knock-down of *TOP2A* in human lung cancer cell lines inhibited cell

proliferation, migration and invasion, while the inhibition of *TOP2A* reduced the expression levels of *CCNB1* and *CCNB2*. High expression of *TOP2A* has been reported to significantly increase the risk of mortality in patients with NSCLC, a risk that is particularly pronounced in patients with LUAD, and its molecular mechanism is associated with activation of PI3K/AKT and Wnt/ β -catenin signaling pathways, which promote apoptosis. Etoposide, which targets *TOP2A*, has been approved for the treatment of small cell lung cancer, but there are currently no drugs for LUAD (48,49). Through various bioinformatics approaches, *TOP2A* has been identified as an independent factor affecting the prognosis of patients with LUAD (50-53), whereas an increased *TOP2A* expression has also been identified as a potential risk factor for pathological stage I LUAD (54). Ciclopirox olamine and quercetin have also been demonstrated to exert tumor-suppressive effects via *TOP2A* in LUAD (55,56).

MELK is highly expressed in LUAD, and the increased expression of *MELK* has been associated with a poor prognosis; *MELK* may serve as a potential diagnostic marker and therapeutic target for LUAD. The molecular mechanisms by which *MELK* affects cancer include the possibility of the kinase activity of *MELK* affecting lung adenocarcinogenesis by inhibiting the pro-apoptotic function of Bcl-GL. High levels

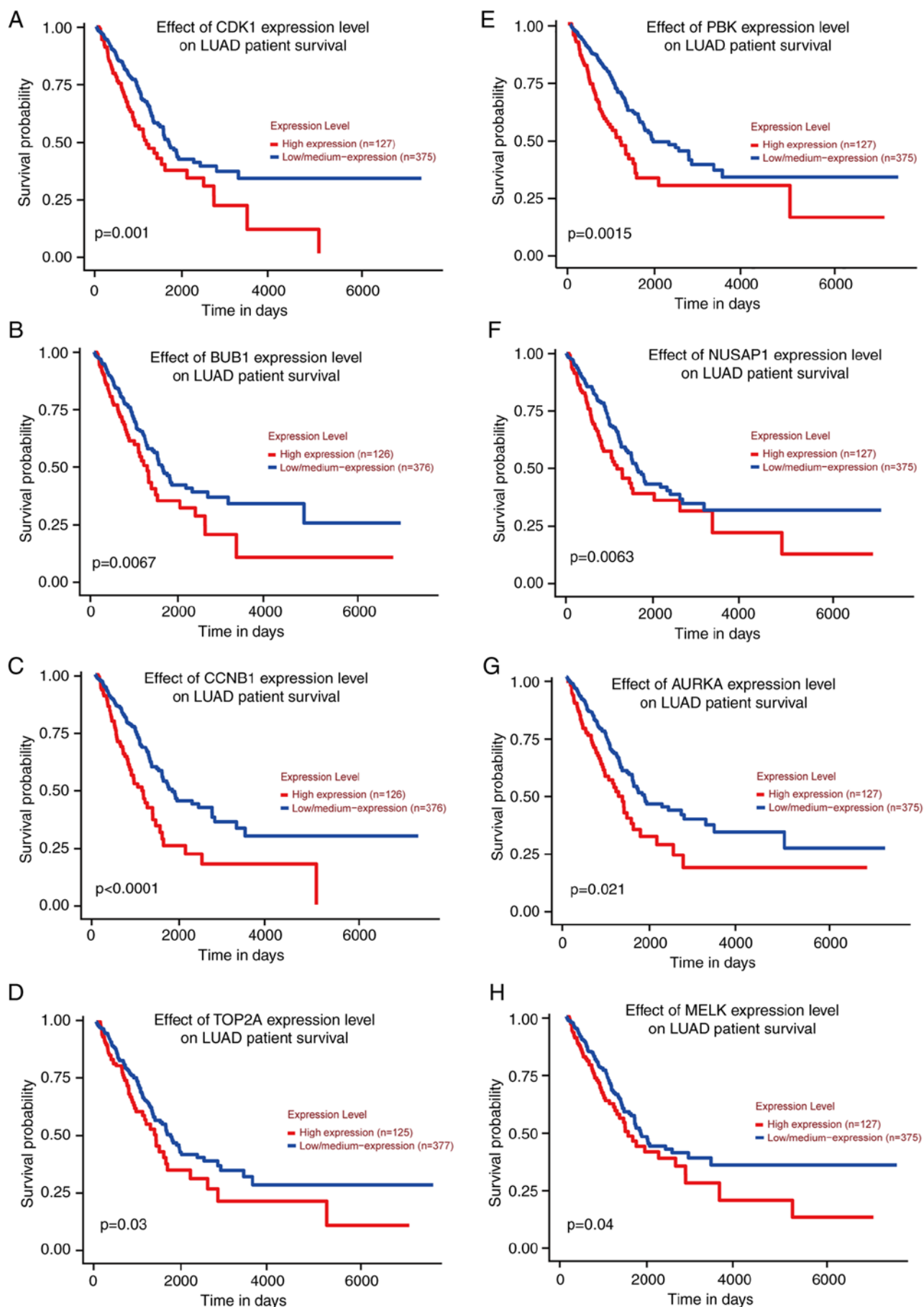


Figure 8. Survival analysis was performed and survival curves were obtained using GEPIA database. According to the P-values, there were eight genes with $P<0.05$ (*AURKA*, *TOP2A*, *CCNB1*, *NUSAP1*, *MELK*, *PBK*, *BUB1* and *CDK1*). (A-H) The survival curves of *CDK1*, *BUB1*, *CCNB1*, *TOP2A*, *PBK*, *NUSAP1*, *AURKA* and *MELK* genes in TCGA database are presented in order. TCGA, The Cancer Genome Atlas.

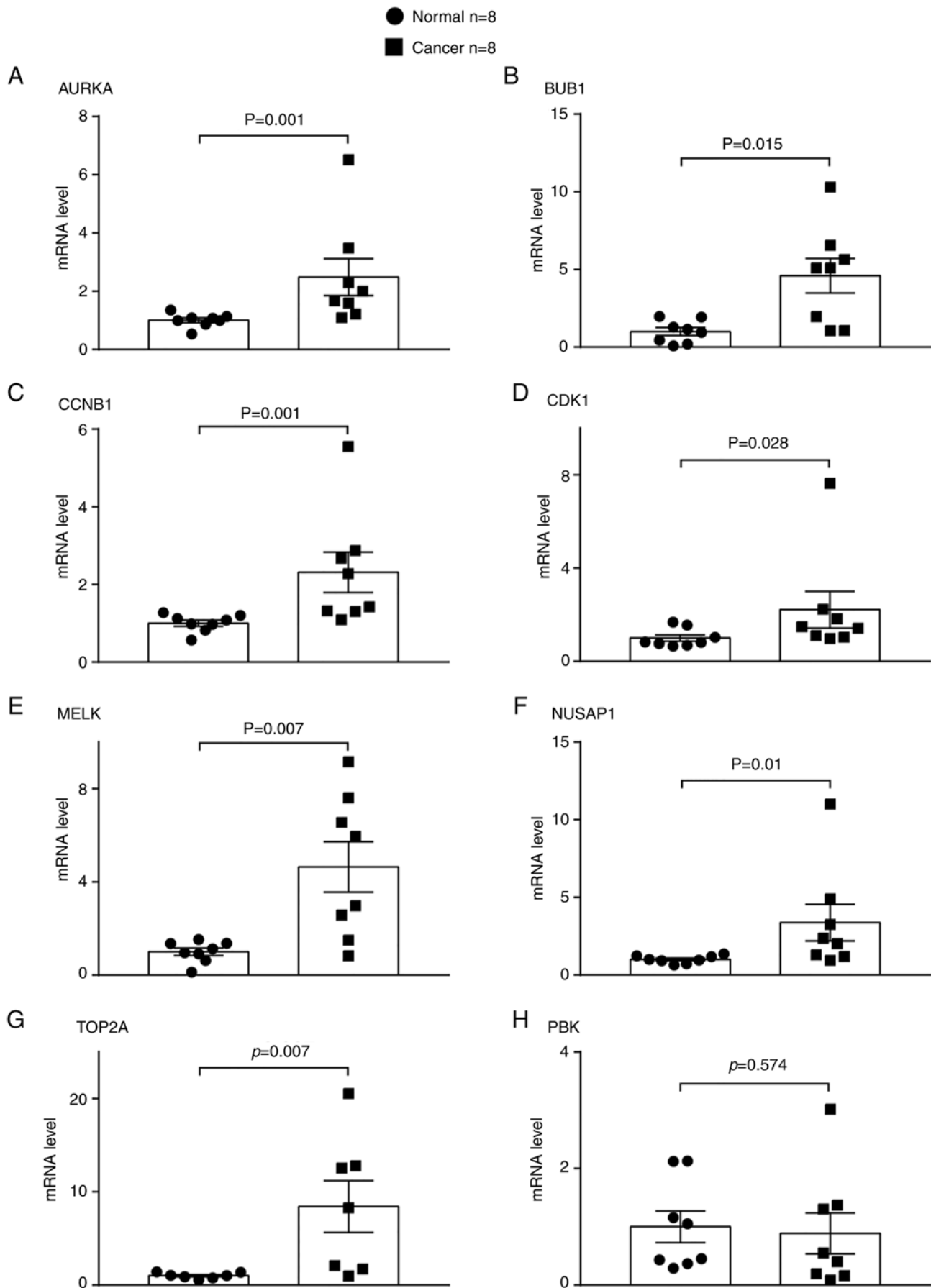


Figure 9. mRNA expression of eight genes screened using WGCNA in clinical tissue samples. Clinical samples are divided into lung adenocarcinoma adjacent tissues and lung adenocarcinoma tissue samples. (A-H) In each graph, the left bar represents the lung adenocarcinoma adjacent tissues, and the right bar the lung adenocarcinoma tissues. The mRNA expression levels of *AURKA*, *BUB1*, *CCNB1*, *CDK1*, *MELK*, *NUSAP1* and *TOP2A* genes in lung adenocarcinoma were higher than those in paired adjacent normal tissues. WGCNA, weighted gene co-expression network analysis.

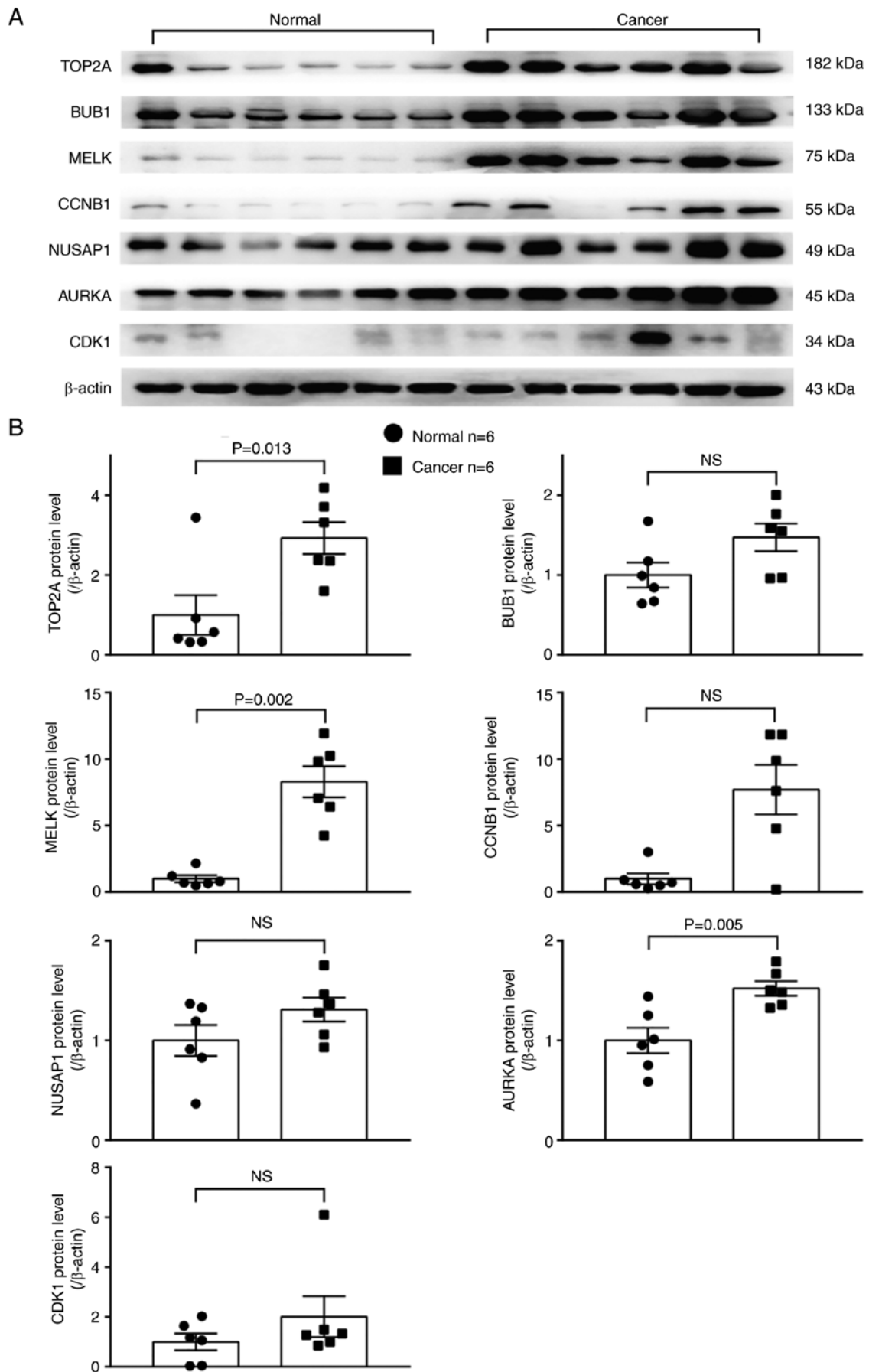


Figure 10. Protein expression of seven genes screened using WGCNA in clinical tissue samples. (A) Representative western blots of AURKA, BUB1, CCNB1, CDK1, MELK, NUSAP1 and TOP2A protein expression in adjacent lung adenocarcinoma tissues and lung adenocarcinoma tissue samples. (B) The quantitative analysis of the data in panel A, in which the protein levels of AURKA, TOP2A and MELK in lung adenocarcinoma tissues were higher than those in matched adjacent lung adenocarcinoma tissues. WGCNA, weighted gene co-expression network analysis.

of *MELK* expression have been associated with high-grade tumors, an increased aggressiveness, a poorer patient prognosis and radioresistance, and an increased expression of *MELK* is associated with *TOP2A*, *CDK1* and *AURKB* (57). Various *MELK* inhibitors have been developed as potential cancer therapeutic agents, molecules, including OTS and MELK-T1 have demonstrated efficacy in experimental animals to delay the proliferation of cancer cells (58).

It has been reported that *TOP2A* interacts directly with *MELK*, *CDC20*, *CCNB2*, *UBE2T*, *KIAA0101* and *TK1* through a PPI network (11). However, this cannot systematically reflect the interaction pattern between key pathogenic genes in LUAD. In the present study, bioinformatics analysis of LUAD using WGCNA and validation by human tissue samples yielded three key genes, *AURKA*, *MELK* and *TOP2A*, whose co-expression may be important for early diagnosis and prognosis as well as further elucidation of the pathogenesis of LUAD.

Acknowledgements

Not applicable.

Funding

The present study was supported by the seventh batch of young and middle-aged medical backbone talent training projects in Wuhan in 2019 [Wu Weitong (2019); Grant no. 87]; National Natural Science Foundation Youth Project (Grant no. 82170106).

Availability of data and materials

The datasets used and/or analyzed during the present study are available from the corresponding author on reasonable request.

Authors' contributions

XZ and YX contributed significantly to the concept and design of the study. XZ and SW conducted bioinformatics experiments and obtained data. HL, RH and MZ conducted confirmatory experiments and obtained data. XZ and JR and LC analyzed the data. XZ, YX and MZ drafted the manuscript. YX, SW and RH critically modify the important intellectual content of the study. XZ and YX confirm the authenticity of all the raw data. BX and NZ and WS contributed to the collection and collation of clinical samples from lung adenocarcinoma patients. All authors have read and approved the final manuscript and have agreed to take responsibility for all aspects of the work.

Ethics approval and consent to participate

The present study was approved (approval no. WDRY2022-K231) by Renmin Hospital of Wuhan University (Wuhan, China) and written informed consent was obtained from patients in all cases.

Patient consent for publication

Not applicable.

Competing interests

The authors declare that they have no competing interests.

References

1. Sung H, Ferlay J, Siegel RL, Laversanne M, Soerjomataram I, Jemal A and Bray F: Global Cancer Statistics 2020: GLOBOCAN estimates of incidence and mortality worldwide for 36 cancers in 185 countries. *CA Cancer J Clin* 71: 209-249, 2021.
2. Denisenko TV, Budkevich IN and Zhivotovsky B: Cell death-based treatment of lung adenocarcinoma. *Cell Death Dis* 9: 117, 2018.
3. Yu Y, Wang Z, Zheng Q and Li J: FAM72 serves as a biomarker of poor prognosis in human lung adenocarcinoma. *Aging (Albany NY)* 13: 8155-8176, 2021.
4. Wang C, Tan S, Liu WR, Lei Q, Qiao W, Wu Y, Liu X, Cheng W, Wei YQ, Peng Y and Li W: RNA-Seq profiling of circular RNA in human lung adenocarcinoma and squamous cell carcinoma. *Mol Cancer* 18: 134, 2019.
5. Li Y, Yu X, Zhang Y, Wang X, Zhao L, Liu D, Zhao G, Gao X, Fu J, Zang A and Jia Y: Identification of a novel prognosis-associated ceRNA network in lung adenocarcinoma via bioinformatics analysis. *Biomed Eng Online* 20: 117, 2021.
6. Li H, Guo L and Cai Z: TCN1 is a potential prognostic biomarker and correlates with immune infiltrates in lung adenocarcinoma. *World J Surg Oncol* 20: 83, 2022.
7. Yuanhua L, Pudong Q, Wei Z, Yuan W, Delin L, Yan Z, Geyu L and Bo S: TFAP2A Induced KRT16 as an Oncogene in Lung Adenocarcinoma via EMT. *Int J Biol Sci* 15: 1419-1428, 2019.
8. Liu ZP: Reverse engineering of genome-wide gene regulatory networks from gene expression data. *Curr Genomics* 16: 3-22, 2015.
9. Langfelder P and Horvath S: WGCNA: An R package for weighted correlation network analysis. *BMC Bioinformatics* 9: 559, 2008.
10. Liu Z, Li M, Fang X, Shen L, Yao W, Fang Z, Chen J, Feng X, Hu L, Zeng Z, *et al*: Identification of surrogate prognostic biomarkers for allergic asthma in nasal epithelial brushing samples by WGCNA. *J Cell Biochem* 120: 5137-5150, 2019.
11. Dong S, Men W, Yang S and Xu S: Identification of lung adenocarcinoma biomarkers based on bioinformatic analysis and human samples. *Oncol Rep* 43: 1437-1450, 2020.
12. Zhang L, He M, Zhu W, Lv X, Zhao Y, Yan Y, Li X, Jiang L, Zhao L, Fan Y, *et al*: Identification of a panel of mitotic spindle-related genes as a signature predicting survival in lung adenocarcinoma. *J Cell Physiol* 235: 4361-4375, 2020.
13. Wang L, Li S, Wang Y, Tang Z, Liu C, Jiao W and Liu J: Identification of differentially expressed protein-coding genes in lung adenocarcinomas. *Exp Ther Med* 19: 1103-1111, 2020.
14. Li J, Liu X, Cui Z and Han G: Comprehensive analysis of candidate diagnostic and prognostic biomarkers associated with lung adenocarcinoma. *Med Sci Monit* 26: e922070, 2020.
15. Wang Y, Zhou Z, Chen L, Li Y, Zhou Z and Chu X: Identification of key genes and biological pathways in lung adenocarcinoma via bioinformatics analysis. *Mol Cell Biochem* 476: 931-939, 2021.
16. Chen C, Tang Y, Qu WD, Han X, Zuo JB, Cai QY, Xu G, Song YX and Ke XX: Evaluation of clinical value and potential mechanism of MTFR2 in lung adenocarcinoma via bioinformatics. *BMC Cancer* 21: 619, 2021.
17. Fan X, Wang Y and Tang XQ: Extracting predictors for lung adenocarcinoma based on Granger causality test and stepwise character selection. *BMC Bioinformatics* 20 (Suppl 7): S197, 2019.
18. Guo W, Sun S, Guo L, Song P, Xue X, Zhang H, Zhang G, Wang Z, Qiu B, Tan F, *et al*: Elevated TOP2A and UBE2C expressions correlate with poor prognosis in patients with surgically resected lung adenocarcinoma: A study based on immunohistochemical analysis and bioinformatics. *J Cancer Res Clin Oncol* 146: 821-841, 2020.
19. Du R, Huang C, Liu K, Li X and Dong Z: Targeting AURKA in Cancer: Molecular mechanisms and opportunities for Cancer therapy. *Mol Cancer* 20: 15, 2021.
20. Meng J, Wei Y, Deng Q, Li L and Li X: Study on the expression of TOP2A in hepatocellular carcinoma and its relationship with patient prognosis. *Cancer Cell Int* 22: 29, 2022.
21. Zhang Y, Yang H, Wang L, Zhou H, Zhang G, Xiao Z and Xue X: TOP2A correlates with poor prognosis and affects radioresistance of medulloblastoma. *Front Oncol* 12: 918959, 2022.

22. Zhang F and Wu H: MiR-599 targeting TOP2A inhibits the malignancy of bladder cancer cells. *Biochem Biophys Res Commun* 570: 154-161, 2021.
23. Gao Y, Zhao H, Ren M, Chen Q, Li J, Li Z, Yin C and Yue W: TOP2A promotes tumorigenesis of high-grade serous ovarian cancer by regulating the TGF- β /Smad pathway. *J Cancer* 11: 4181-4192, 2020.
24. Wang B, Shen Y, Zou Y, Qi Z, Huang G, Xia S, Gao R, Li F and Huang Z: TOP2A promotes cell migration, invasion and epithelial-mesenchymal transition in cervical cancer via activating the PI3K/AKT signaling. *Cancer Manag Res* 12: 3807-3814, 2020.
25. Pei YF, Yin XM and Liu XQ: TOP2A induces malignant character of pancreatic cancer through activating β -catenin signaling pathway. *Biochim Biophys Acta Mol Basis Dis* 1864: 197-207, 2018.
26. Chen YU, Yu Y, Lv M, Shi Q and Li X: E2F1-mediated up-regulation of TOP2A promotes viability, migration, and invasion, and inhibits apoptosis of gastric cancer cells. *J Biosci* 47: 84, 2022.
27. Du X, Xue Z, Lv J and Wang H: Expression of the topoisomerase II alpha (TOP2A) gene in lung adenocarcinoma cells and the association with patient outcomes. *Med Sci Monit* 26: e929120, 2020.
28. Chen C, Guo Q, Song Y, Xu G and Liu L: SKA1/2/3 serves as a biomarker for poor prognosis in human lung adenocarcinoma. *Transl Lung Cancer Res* 9: 218-231, 2020.
29. Gray D, Jubb AM, Hogue D, Dowd P, Kljavin N, Yi S, Bai W, Frantz G, Zhang Z, Koeppen H, *et al*: Maternal embryonic leucine zipper kinase/murine protein serine-threonine kinase 38 is a promising therapeutic target for multiple cancers. *Cancer Res* 65: 9751-9761, 2005.
30. Li Y, Li Y, Chen Y, Xie Q, Dong N, Gao Y, Deng H, Lu C and Wang S: MicroRNA-214-3p inhibits proliferation and cell cycle progression by targeting MELK in hepatocellular carcinoma and correlates cancer prognosis. *Cancer Cell Int* 17: 102, 2017.
31. Chen S, Zhou Q, Guo Z, Wang Y, Wang L, Liu X, Lu M, Ju L, Xiao Y and Wang X: Inhibition of MELK produces potential anti-tumour effects in bladder cancer by inducing G1/S cell cycle arrest via the ATM/CHK2/p53 pathway. *J Cell Mol Med* 24: 1804-1821, 2020.
32. Tang Z, Li C, Kang B, Gao G, Li C and Zhang Z: GEPIA: A web server for cancer and normal gene expression profiling and interactive analyses. *Nucleic Acids Res* 45: W98-W102, 2017.
33. Cancer Genome Atlas Research Network; Weinstein JN, Collisson EA, Mills GB, Shaw KR, Ozenberger BA, Ellrott K, Shmulevich I, Sander C and Stuart JM: The Cancer Genome Atlas Pan-Cancer analysis project. *Nat Genet* 45: 1113-1120, 2013.
34. Livak KJ and Schmittgen TD: Analysis of relative gene expression data using real-time quantitative PCR and the 2(-Delta Delta C(T)) method. *Methods* 25: 402-408, 2001.
35. Allemani C, Matsuda T, Di Carlo V, Harewood R, Matz M, Nikšić M, Bonaventure A, Valkov M, Johnson CJ, Estève J, *et al*: Global surveillance of trends in cancer survival 2000-14 (CONCORD-3): Analysis of individual records for 37 513 025 patients diagnosed with one of 18 cancers from 322 population-based registries in 71 countries. *Lancet* 391: 1023-1075, 2018.
36. Zhao X, Zhang L, Wang J, Zhang M, Song Z, Ni B and You Y: Identification of key biomarkers and immune infiltration in systemic lupus erythematosus by integrated bioinformatics analysis. *J Transl Med* 19: 35, 2021.
37. Hu X, Bao M, Huang J, Zhou L and Zheng S: Identification and validation of novel biomarkers for diagnosis and prognosis of hepatocellular carcinoma. *Front Oncol* 10: 541479, 2020.
38. Yang Q, Wang R, Wei B, Peng C, Wang L, Hu G, Kong D and Du C: Candidate biomarkers and molecular mechanism investigation for glioblastoma multiforme utilizing WGCNA. *Biomed Res Int* 2018: 4246703, 2018.
39. Vernocchi P, Gili T, Conte F, Del Chierico F, Conta G, Miccheli A, Botticelli A, Paci P, Caldarelli G, Nuti M, *et al*: Network analysis of gut microbiome and metabolome to discover microbiota-linked biomarkers in patients affected by non-small cell lung cancer. *Int J Mol Sci* 21: 8730, 2020.
40. Otto T and Sicinski P: Cell cycle proteins as promising targets in cancer therapy. *Nat Rev Cancer* 17: 93-115, 2017.
41. Li Z, Zhang Y, Zhou Y, Wang F, Yin C, Ding L and Zhang S: Tanshinone IIA suppresses the progression of lung adenocarcinoma through regulating CCNA2-CDK2 complex and AURKA/PLK1 pathway. *Sci Rep* 11: 23681, 2021.
42. Zhong N, Shi S, Wang H, Wu G, Wang Y, Ma Q, Wang H, Liu Y and Wang J: Silencing Aurora-A with siRNA inhibits cell proliferation in human lung adenocarcinoma cells. *Int J Oncol* 49: 1028-1038, 2016.
43. Zhang MY, Liu XX, Li H, Li R, Liu X and Qu YQ: Elevated mRNA Levels of AURKA, CDC20 and TPX2 are associated with poor prognosis of smoking related lung adenocarcinoma using bioinformatics analysis. *Int J Med Sci* 15: 1676-1685, 2018.
44. Yang PJ, Hsieh MJ, Lee CI, Yen CH, Wang HL, Chiang WL, Liu TC, Tsao TC, Lee CY and Yang SF: Impact of aurora kinase a polymorphism and epithelial growth factor receptor mutations on the clinicopathological characteristics of lung adenocarcinoma. *Int J Environ Res Public Health* 17: 7350, 2020.
45. Zheng X, Chi J, Zhi J, Zhang H, Yue D, Zhao J, Li D, Li Y, Gao M and Guo J: Aurora-A-mediated phosphorylation of LKB1 compromises LKB1/AMPK signaling axis to facilitate NSCLC growth and migration. *Oncogene* 37: 502-511, 2018.
46. Shah KN, Bhatt R, Rotow J, Rohrberg J, Olivas V, Wang VE, Hemmati G, Martins MM, Maynard A, Kuhn J, *et al*: Aurora kinase A drives the evolution of resistance to third-generation EGFR inhibitors in lung cancer. *Nat Med* 25: 111-118, 2019.
47. Gao J, Lu F, Yan J, Wang R, Xia Y, Wang L, Li L, Chang L and Li W: The role of radiotherapy-related autophagy genes in the prognosis and immune infiltration in lung adenocarcinoma. *Front Immunol* 13: 992626, 2022.
48. Grenda A, Błach J, Szczyrek M, Krawczyk P, Nicoś M, Kuźnar Kamińska B, Jakimiec M, Balicka G, Chmielewska I, Batura-Gun H, *et al*: Promoter polymorphisms of TOP2A and ERCC1 genes as predictive factors for chemotherapy in non-small cell lung cancer patients. *Cancer Med* 9: 605-614, 2020.
49. Kou F, Sun H, Wu L, Li B, Zhang B, Wang X and Yang L: TOP2A promotes lung adenocarcinoma cells' malignant progression and predicts poor prognosis in lung adenocarcinoma. *J Cancer* 11: 2496-2508, 2020.
50. Zeng H, Ji J, Song X, Huang Y, Li H, Huang J and Ma X: Stemness related genes revealed by network analysis associated with tumor immune microenvironment and the clinical outcome in lung adenocarcinoma. *Front Genet* 11: 549213, 2020.
51. Song Y, Tang W and Li H: Identification of KIF4A and its effect on the progression of lung adenocarcinoma based on the bioinformatics analysis. *Biosci Rep* 41: BSR20203973, 2021.
52. Dai JJ, Zhou WB and Wang B: Identification of crucial genes associated with lung adenocarcinoma by bioinformatic analysis. *Medicine (Baltimore)* 99: e23052, 2020.
53. Zhang S, Pang K, Feng X and Zeng Y: Transcriptomic data exploration of consensus genes and molecular mechanisms between chronic obstructive pulmonary disease and lung adenocarcinoma. *Sci Rep* 12: 13214, 2022.
54. Deng Y, Chen X, Huang C, Song J, Feng S, Chen X and Zhou R: Screening and validation of significant genes with poor prognosis in pathologic Stage-I lung adenocarcinoma. *J Oncol* 2022: 3794021, 2022.
55. Yin J, Che G, Jiang K, Zhou Z, Wu L, Xu M, Liu J and Yan S: Ciclopirox olamine exerts tumor-suppressor effects via topoisomerase II alpha in lung adenocarcinoma. *Front Oncol* 12: 791916, 2022.
56. Zhang YQ, Li K, Guo Q and Li D: A new risk model based on 7 quercetin-related target genes for predicting the prognosis of patients with lung adenocarcinoma. *Front Genet* 13: 890079, 2022.
57. Du T, Qu Y, Li J, Li H, Su L, Zhou Q, Yan M, Li C, Zhu Z and Liu B: Maternal embryonic leucine zipper kinase enhances gastric cancer progression via the FAK/Paxillin pathway. *Mol Cancer* 13: 100, 2014.
58. McDonald IM and Graves LM: Enigmatic MELK: The controversy surrounding its complex role in cancer. *J Biol Chem* 295: 8195-8203, 2020.



This work is licensed under a Creative Commons Attribution-NonCommercial-NoDerivatives 4.0 International (CC BY-NC-ND 4.0) License.